PCCP

Accepted Manuscript

ROYAL SOCIETY OF CHEMISTRY

www.rsc.org/pccp

Excited-state Hydrogen-bonding Dynamics of Camphorsulfonic Acid Doped Polyaniline: A Theoretical Study

Yahong Zhang, Yuping Duan *, Tongmin Wang

School of Materials Science and Engineering, Dalian University of Technology, Dalian116085, PR China

Abstract

The first-principles calculation was performed to study the hydrogen bond in camphorsulfonic (CSA) acid-doped polyaniline system. The density functional theory (DFT) method was used to calculate the ground-state geometric structure optimization. Meanwhile, the electronic excitation energies and corresponding oscillation strengths of the low-lying electronically excited states were investigated by time-dependent density functional theory (TDDFT) method. In the acid-doped system, the S=O···H-N type intermolecular hydrogen bonds were formed. The band lengths at the hydrogen bond formation point were elongated, and the stronger hydrogen-bond interaction cause the longer bond stretching. The DPA-DMSO was photoexcited to S2 state which possessed the largest oscillator strength, and the ICPA-DMSO was photoexcited to the S3 state in the similar way. In addition, we also discussed the frontier molecular orbitals and the electron density transition.

Key words: hydrogen bond, excited states, TDDFT, molecular orbitals

1. Introduction

The solute solvent interactions play an important role in molecular nonequilibrium process and have been a key point of solution chemistry.[1-5] Intermolecular hydrogen bonding, as the interaction between hydrogen donor and acceptor molecules, is an important type of site-specific solute-solvent interaction.[6,7] Furthermore, the hydrogen bonding interaction also makes a contribution to the

*Corresponding author. Tel: +86-411-84708446; fax: +86-411-84708446
E-mail address: duanyp@dlut.edu.cn

understanding of microscopic structure and function in many molecular systems.[8,9] In the last few years, as scientists have recognized the importance of hydrogen bonding in the physics, chemistry and biology fields, they used a variety of experimental and theoretical methods to investigate the hydrogen bond (H-band) between molecules. Thus, the hydrogen bonding has been studied extensively which has a effect on the structures, electronic properties and dynamics of many important molecular systems.[10-12] Based on the preceding research for electronic ground-state properties of intermolecular hydrogen bonding, the investigation of H-band in the electronically excited states should be carried out significantly.

The charge distribution of H-band will be changed in the different electronic excited states by photoexcitation. The changing process is known as the electronic excited-state hydrogen bonding dynamics, and it always occurs on ultrafast time scales mainly set by vibrational motions of hydrogen donor and acceptor groups.[13,14] The phenomenon that electronic spectral shifts are significantly associated with electronic excited-state hydrogen-bonding dynamics has been described clearly by Zhao and Han.[14,15] The relationship between the hydrogen-bonding dynamics and electronic spectra is that hydrogen bond strengthening will make the relative electronic spectra shift to red. Conversely, hydrogen bond weakening can cause the electronic spectra blueshift (shown as Fig. 1). In recent years, more and more attentions have been paid to the hydrogen-bonding dynamics for the reason that significant strengthening or weakening of hydrogen bond in the electronically excited states is tightly associated with many photochemical, photophysical and photobiological phenomena such as fluorescence quenching and photo-induced electron transfer. [16-19]

Polyaniline (PANi) with unique conducting and optical property remains one of the most intensely studied conjugated polymers.[20,21] Despite its long history, the interest shown in PANi has continued to increase in recent years.[22] This is partly due to its high chemical and environmental stability, the simple and cheap preparation process, and amazing electrical conductivity shown by its salt. The early studies of PANi were mostly focused on the synthesis experiment and the performance analysis

as well as the H-band interaction. Nowadays more and more theoretical methods were used to investigate the structure and energetics of various aspects of PANi.[23-26] Further more, most of recent papers have applied DFT methods to the study of PANi and concluded that these methods are suitable for the modeling. For instance, the doping process of PANi has been investigated using DFT methods,[27-29] and the theoretical calculation of hydrogen bonding in PANi has been carried out as well, [23,30] and the investigations were mainly focused on the structural and electronic influences on the hydrogen bonding complexes. However, as far as we know, there are few investigations about the hydrogen-bonding dynamics of hydrogen-bonded PANi acid complexes in electronically excited states. Hence, the study of hydrogen-bonding dynamics in electronically excited states of PANi acid complexes is important.

Based on the above, in this paper, the ground-state geometric structures of hydrogen-bonded complexes were optimized. Furthermore, the electronic excitation energies and the corresponding oscillation strengths of the configurations in their low-lying electronically excited states were calculated. In addition, the electron density transition and the frontier molecular orbitals (MOs) were also analyzed.

2. Model and Method

Because the complexes of PANi and CSA contain too many atoms to be modeled by DFT method effectively, we have to choose a series of smaller molecule models to represent the most important functional groups and interactions presented in the PANi and CSA structure. And the selected model compounds have been proven to be reasonable by Joel.[23] The Ph_2NH (DPA) and (4-iminocyclohexa-2, 5-dienylidene) phenylamine cation (ICPA) are used to model the distinct amine and iminium nitrogen cation environments in ES respectively, while CSA is modeled by dimethylsulfoxide (DMSO), and the H-bond can be formed between the S=O group of DMSO and the H-N groups of DPA as well as ICPA monomers, which are denoted as DPA-DMSO and ICPA-DMSO hydrogen-bonded complexes respectively. The chemical structures of the monomers as well as the hydrogen-bonded complexes are shown in Fig. 2.

All the electronic structure calculations were carried out using the Gaussian 09 program suite. The ground-state geometric optimization of the isolated DPA, ICPA and DMSO monomers as well as the hydrogen-bonded DPA-DMSO and ICPA-DMSO complexes considered here were carried out using DFT with the B3LYP hybrid functional. The electronic transition energies and corresponding oscillation strengths of all the hydrogen-bonded complexes in their low-lying electronically excited states were calculated using TDDFT with the B3LYP hybrid functional method. The 6-31G+(d, p) was chosen as basis set throughout the whole process.

3. Results and Discussion

3.1. Equilibrium geometries of the ground state

As we know, the H-bond is the bond between electron-deficient hydrogen and a region of high electron density. The most common H-bond is the X-H⋯Y type, where X and Y are electronegative elements and Y possesses one or more lone electron pairs. The N-H group of DPA and ICPA as well as the S=O group of DMSO are the possible sites that are responsible for hydrogen bond formation between DPA/ICPA and DMSO monomers. Thus, the possible conformations of the hydrogen-bonded DPA-DMSO and ICPA-DMSO complexes are investigated. The equilibrium geometries of the hydrogen-bonded DPA-DMSO and ICPA-DMSO complexes as well as the involved monomers in ground state are shown in Fig. 3, and the important structure parameters are collected in Table 1. The bond lengths of C6-N1 and C8=N1 groups in the DPA-DMSO or ICPA-DMSO hydrogen-bonded complexes are all shortened compared with their lengths in the DPA and ICPA monomers. The C8=N1 possess relative small bond length value both in ICPA monomer and ICPA-DMSO complexes, which is responsible for the double bond character. The bond lengths of C13-S1 and C14-S1 groups in the hydrogen-bonded complexes show the shortened tendency compared with their lengths in the DMSO monomer. The valence angle of C6-N1-C8 in the DPA-DMSO and ICPA-DMSO complexes are 129.1043°, 128.1074° respectively, which are all decreased compared with their value in the monomers, but the valence angle of C13-S1-C14 shows the opposite character that it

is increased in the complexes. As shown in Fig. 3, the intermolecular hydrogen bonds O1-H11 between H and O atoms can be clearly seen in DPA-DMSO and ICPA-DMSO hydrogen-bonded complexes. The lengths of the H-bond S1=O1···H11-N1 in DPA-DMSO and ICPA-DMSO complexes are 1.9680 Å and 1.6482Å respectively, and the shorter H-bond in ICPA-DMSO complex will show relative stronger hydrogen-bond interaction. There is an obvious phenomenon that the bond lengths of H11-N1 and S1-O1 in the complexes are all elongated simultaneously, and the stronger hydrogen-bond interaction causes much more obvious stretch. In other words, when the atoms are involved in the formation of the hydrogen bond the bands connected by these atoms will be elongated.

3.2. Nature of low-lying excited states

It is necessary to understand the nature of the low-lying electronically excited states before the discussion of excited states for DPA/ICPA monomers and their hydrogen-bonded complexes. We calculated the electronic excitation energies and the oscillation strengths of the DPA-DMSO, ICPA-DMSO hydrogen-bonded complexes as well as the isolated DPA, ICPA monomers using the TDDFT method. The results are collected in Table 2. The oscillator strength is a dimensionless quantity to express the strength of the transition. The S2 state of the hydrogen-bonded DPA-DMSO complex possesses the largest oscillator strength. As a result, the DPA-DMSO complex will be photoexcited to the S2 state directly. It is obvious that the S1-S8 states electronic excitation energies of the DPA-DMSO complex are lower compared with the correspond states of the DPA monomer. We can draw the conclusion that the intermolecular hydrogen bonding S1=O1···H11–N1 is strengthened for the S1-S8 states of the DPA-DMSO complex and can induce a redshift. In ICPA-DMSO complex, all the electronic excitation energies of the calculated excited states except for the S1-S3 states are under those of the ICPA monomer, therefore, the hydrogen bond S1=O1···H11–N1 in the ICPA-DMSO complex is strengthened for the S4-S8 states and will bring a redshift. On the contrary, the electronic spectra of the S1-S3 states are shifted towards blue due to the weakened hydrogen bond. Furthermore, the ICPA-DMSO hydrogen complex maybe primarily excited to the S3 state on account

of its largest oscillator strength.

3.3. Infrared spectra and vibration model

The infrared spectra and vibration model of the isolated DPA, ICPA monomers as well as the hydrogen-bonded DPA-DMSO, ICPA-DMSO complexes are calculated as shown in Fig. 4. The study is focused on the spectra and vibration of N–H bands in the monomers and the complexes. From Fig. 4(a), it's easy to see that the presence of N–H absorption peak at 3635 cm^{-1} in DPA monomer shifts to 3475cm^{-1} in DPA-DMSO complex, and the intensity of the vibration is enhanced in the complex. From Fig. 4(b), we can draw the quite similar conclusion that the N–H absorption peak of ICPA-DMSO complex is also enhanced and shifts to 2895cm^{-1} from 3542cm^{-1} compared with ICPA monomer. The vibration model of the isolated monomers and the hydrogen-bonded complexes are simulated as shown in Fig. 4(c,d), and it's obvious that the N–H band is off-plane swing vibration in DPA monomer but is in-plane stretching vibration in DPA-DMSO complex. At the same time, the N–H band is in-plane stretching vibration in both ICPA monomer and ICPA-DMSO complex.

3.4. Frontier Molecular Orbitals (MOs)

The analysis of MOs will contribute to further understanding for the nature of the excited states. As mentioned before, our discussion has been focused on the S2 state of hydrogen-bonded DPA-DMSO complex and the S3 state of ICPA-DMSO hydrogen complex. The two states of the DPA-DMSO and ICPA-DMSO complexes are associated with the HOMO and LUMO orbitals. The frontier molecular orbitals of the DPA-DMSO and ICPA-DMSO complexes as well as the DPA and ICPA monomers are shown in Fig. 5, and only the HOMO and LUMO orbitals are presented. From the MOs of DPA-DMSO, it's easy to see that the HOMO orbital possessed the π character, and the LUMO orbital showed the π^* character. As a result, from HOMO to LUMO will be a π-π^* transition. It is obvious that in the MOs of ICPA-DMSO, the electron density is focused on benzenoid ring in HOMO orbital, whereas the quinoid ring in LUMO orbital possesses more electron density, and the electron density transfers from benzenoid ring to quinoid ring during the HOMO to LUMO orbital transition. In addition, it's obvious that the electronic densities of the complex orbitals are mainly

distributed on the DPA and ICPA chain. Therefore, for the hydrogen-bonded DPA-DMSO and ICPA-DMSO complexes, only the electrons of the DPA and ICPA monomers are excited in these states, whereas the DMSO monomer remains in its electronic ground state.

4. Conclusions

In conclusion, there were two possible hydrogen bond interactions between DPA/ICPA and DMSO monomers, and the geometric structures were affected by the formation of hydrogen bond, especially the H11-N1 and S1-O1 bonds involved in forming the hydrogen bond, and the stronger hydrogen-bond interaction caused the more obvious band stretch. According to the result of comparing oscillator strength, the DPA-DMSO and ICPA-DMSO complexes were excited to S2 and S3 states respectively. The hydrogen-bond interaction brought the significant redshift of N–H band in the complexes, and the vibration models were also affected by hydrogen-bond formation, especially the N–H band. The S2 state of DPA-DMSO was due to a distinct π-π^* feature, meanwhile there was obvious intramolecular electron density transfer in ICPA-DMSO during the orbital transition from HOMO to LUMO, and the hydrogen bonds were strongly influenced by the charge redistribution which was involved in the orbital transition. Moreover, we noted the phenomenon that only the DPA and ICPA molecules were excited in these states, and the DMSO was stayed in its ground state.

Acknowledgements

The authors acknowledge the Supported by Program for New Century Excellent Talents in University [No. NCET-13-0071], the National Science and Technology support plan for twelfth five years of China [No: 2012BAJ02B04], and the Fundamental Research Funds for the Central Universities (DUT14YQ201), the Natural Science Foundation of Liaoning Province [No. 2013020098].

References

1. R. Jimenez, G. R. Fleming, P. V. Kumar and M. Maroncelli, *Nature*, 1994, **369**, 471-473

2. S. Woutersen, U. Emmerichs and H. J. Bakker, *Science*, 1997, **278**, 658-660

3. R. Adhikary, P. Mukherjee, T. W. Kee and J. W. Petrich, *J. Phys. Chem. B*, 2009, **113**, 5255-5261

4. S. Abbruzzetti, E. Grandi, C. Viappiani, B. Sara, C. Barbara, R. Samanta, B. Stefano and M. Andrea, *J. Am. Chem. Soc.*, 2005, **127**, 626-635

5. A. Patra, T. Q. Luong, R. K. Mitra, M. Havenith, *Phys. Chem. Chem. Phys.*, 2013, **15**, 930-939

6. J. A. Gutierrez , R. D. Falcone , J. J. Silber and N. M. Correa, *J. Phys. Chem. A*, 2010, **114**, 7326-7330

7. M. Caselli, E. Ferrari, C. Imbriano, F. Pignedoli, M. Saladini and G. Ponterini, *J. Photochem. Photobiol., A*, 2010, **210**, 115-124

8. B. Kuhn, P. Mohr and M. Stahl, *J. Med. Chem.*, 2010, **53**, 2601-2611

9. G. J. Zhao, B. H. Northrop, K. L. Han and P. J. Stang, *J. Phys. Chem. A*, 2010, **114**, 9007-9013

10. Y. Liu, J. Ding, R. Liu, D. Shi and J. Sun, *J. Comput. Chem.*, 2009, **30**, 2723-2727

11. M. Boggio-Pasqua, M. A. Robb and G. Groenhof, *J. Am. Chem. Soc.*, 2009, **131**, 13580-13581

12. Y. H. Liu, G. J. Zhao, G. Y. Li and K. L. Han, *J. Photochem. Photobiol., A*, 2010, **209**, 181-185

13. G. J. Zhao and K. L. Han, *Biophys. J.*, 2008, **94**, 38-46

14. G. J. Zhao and K. L. Han, *ChemPhysChem*, 2008, **9**, 1842-1846

15. G. J. Zhao and K. L. Han, *Acc. Chem. Res.*, 2012, **45**, 404-413

16. G. J. Zhao and K. L. Han, *J. Phys. Chem. A*, 2007, **111**, 2469-2474

17. G. J. Zhao, J. Y. Liu, L. C. Zhou and K. L. Han, *J. Phys. Chem. B*, 2007, **111**, 8940-8945

18. G. J. Zhao, K. L. Han and P. J. Stang, *J. Chem. Theory Comput.*, 2009, **5**, 1955-1958

19. G. J. Zhao and K. L. Han, *J. Phys. Chem. A*, 2009, **113**, 14329-14335

20. A. G. Macdiarmid, J. C. Chiang, A. F. Richter and A. J. Epstein, *Synth. Met.*, 1987, **18**, 285-290

21. W. S. Huang, B. D. Humphrey and A. G. MacDiarmid, *J. Chem. Soc., Faraday Trans. 1 F*, 1986, **82**, 2385-2400

22. M. Jaymand, *Prog. Polym. Sci.*, 2013, **38**, 1287-1306

23. J. P. Foreman and A. P. Monkman, *J. Phys. Chem. A*, 2003, **107**, 7604-7610

24. Z. T. de Oliveira and M. C. Dos Santos, *Chem. Phys.*, 2000, **260**, 95-103

25. A. Varela-Álvarez, J. A. Sordo and G. E. Scuseria, *J. Am. Chem. Soc.*, 2005, **127**, 11318-11327

26. X. Chen , C. A. Yuan, C. K. Y. Wong, H. He, S. Y. Y. Leung and G. Zhang, *Sens. Actuators, B*, 2012, **174**, 210-216

27. J. N. Petrova, J. R. Romanova, G. K. Madjarova, A. N. Ivanova and A. V. Tadjer, *J. Phys. Chem. B*, 2011, **115**, 3765-3776

28. J. Romanova, J. Petrova, A. Ivanova, A. Tadjera and N. Gospodinova, *J. Mol. Struct. THEOCHEM*, 2010, **954**, 36-44

29. J. Romanova, G. Madjarova, A. Tadjer, and N. Gospodinova, *Int. J. Quantum Chem.*, 2011, **111**, 435-443

30. L. W. Shacklette, *Synth. Met.*, 1994, **65**, 123-130

Tables

Table 1. The bond lengths (Å) and bond angles (º) for the isolated monomers and the hydrogen-bonded complexes in their ground states.

	DPA	ICPA	DMSO	DPA-DMSO	ICPA-DMSO
C6-N1	1.4004	1.4305	-	1.3964	1.4264
C8-N1	1.4004	1.3293	-	1.3959	1.3220
H11-N1	1.0092	1.0175	-	1.0189	1.0532
O1-H11	–	–	–	1.9680	1.6482
C13-S1	-	-	1.8363	1.8317	1.8214
C14-S1	-	-	1.8363	1.8304	1.8222
S1-O1	-	-	1.5190	1.5297	1.5499
C13-S1-C14	-	-	96.4773	97.2521	98.5812
C6-N1-C8	129.6500	129.7435	-	129.1043	128.1074

Table 2. The electronic transition energies (eV) and corresponding oscillation strengths (in parentheses) of the isolated monomers and the hydrogen-bonded complexes for the low-lying electronically excited states (R: redshift; B: blueshift).

	DPA	ICPA	DPA-DMSO	ICPA-DMSO
S1	4.1873(0.1055) H->L+1(52%)	2.5555(0.0013) H-1->L(70%)	4.0217(0.0171)R H->L+2(46%)	2.6974(0.0348)B H-1->L(57%)
S2	4.2395(0.2917) H->L (51%)	2.6985(0.3109) H->L (52%)	4.1455(0.2684)R H->L (56%)	2.8581(0.0053)B H-2->L (68%)
S3	4.3224(0.0210) H->L+2(52%)	2.8636(0.0321) H-2->L(52%)	4.2196(0.1258)R H->L+1(41%)	2.9004(0.2292)B H->L (50%)
S4	4.5982(0.0964) H->L+3(68%)	3.6241(0.0099) H-4->L (52%)	4.2838(0.0211)R H->L+3(57%)	3.0435(0.0713)R H-3->L (61%)
S5	5.0717(0.0399) H->L+5(70%)	4.3498(0.4518) H-3->L (54%)	4.3015(0.0270)R H->L+3(59%)	3.6249(0.0084)R H-4->L (58%)
S6	5.0778(0.0003) H->L+4(66%)	5.0512(0.0125) H->L+1(52%)	4.5006(0.0507)R H->L+4(69%)	3.6881(0.0055)R H-6->L (45%)
S7	5.2354(0.0064) H->L+6(63%)	5.0821(0.0032) H-5->L (52%)	4.7581(0.0292)R H->L+6(64%)	4.3890(0.4694)R H-6->L (46%)
S8	5.5357(0.0097) H->L+7(69%)	5.2226(0.0043) H-6->L+1(52%)	4.7828(0.0004)R H->L+5(62%)	5.1311(0.0013)R H-8->L (48%)

Captions for Figures

Figure 1. The schematic diagram of electronic spectral redshift and blueshift induced by the excited state hydrogen bonding dynamics.

Figure 2. The chemical structures of the monomers and the hydrogen-bonded complexes. The dotted lines represent the intermolecular hydrogen bonds.

Figure 3. The geometric structures of monomers and the hydrogen-bonded complexes. The dotted lines represent the intermolecular hydrogen bonds.

Figure 4. The infrared spectra and vibration model of the isolated DPA, ICPA monomers and the hydrogen-bonded DPA-DMSO, ICPA-DMSO complexes.
(a) infrared spectra of DPA and DPA-DMSO; (b) infrared spectra of ICPA and ICPA-DMSO; (c) vibration model of DPA and DPA-DMSO; (d) vibration model of ICPA and ICPA-DMSO.

Figure 5. Frontier molecular orbitals (MOs) of the hydrogen-bonded DPA-DMSO and ICPA-DMSO complexes. The MOs of the isolated DPA and ICPA are also shown for comparation.

Fig. 1

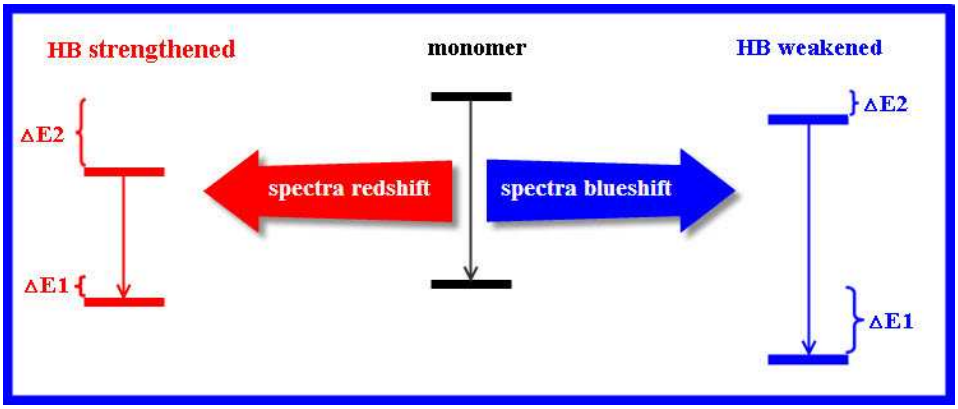

Fig. 2

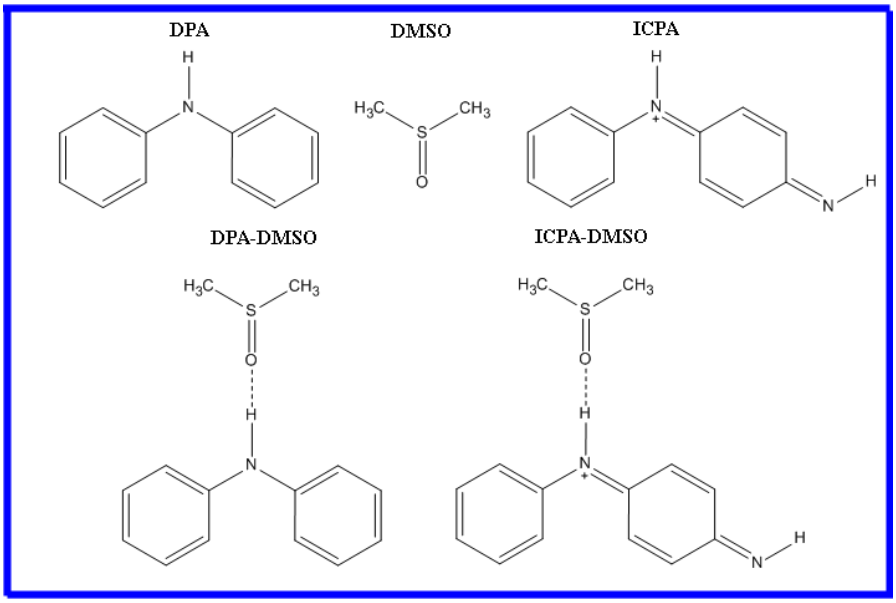

Fig. 3

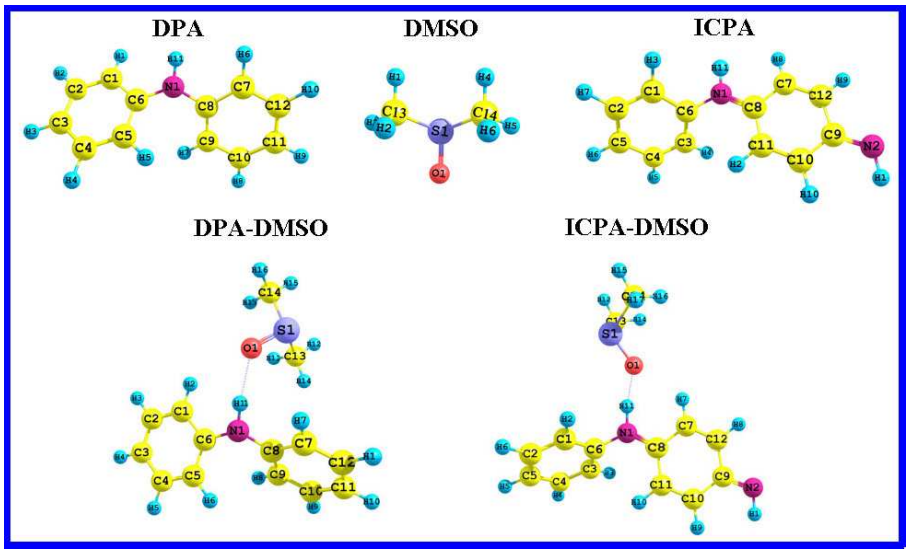

Fig. 4

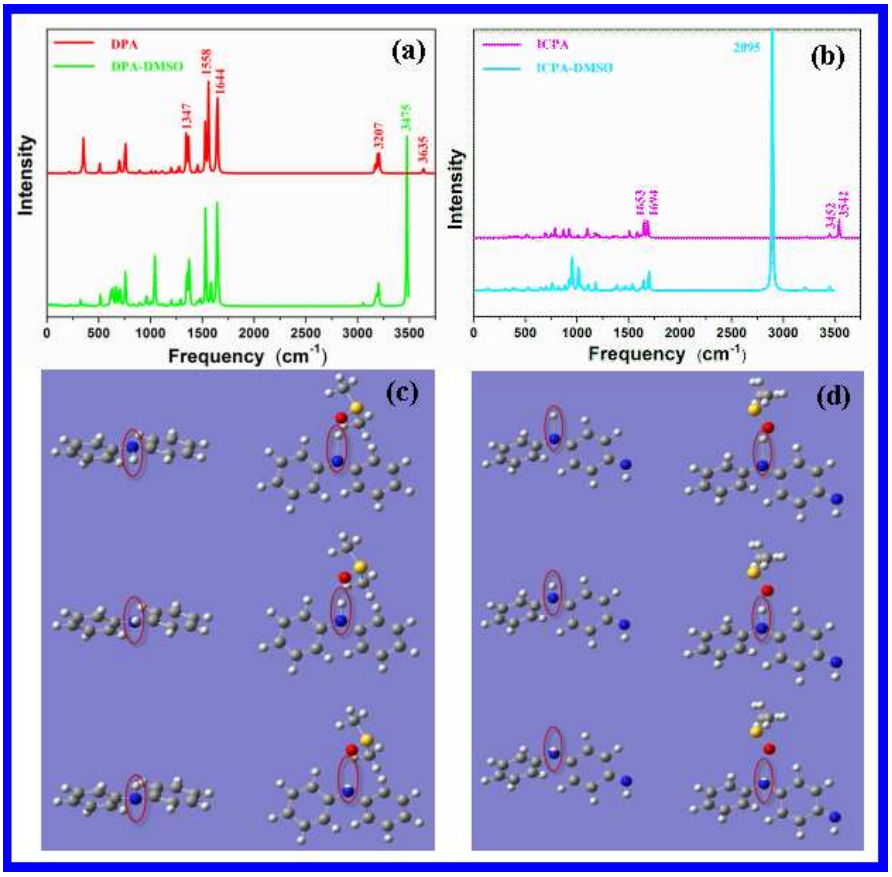

Fig. 5